

PAPER • OPEN ACCESS

Supercritical helium expansivity effects on magnet protection systems

To cite this article: M H Vanderlaan and T J Brumm 2020 *IOP Conf. Ser.: Mater. Sci. Eng.* **755** 012130

View the [article online](#) for updates and enhancements.

Supercritical helium expansivity effects on magnet protection systems

M H Vanderlaan and T J Brumm

National High Magnetic Field Laboratory, 1800 E Paul Dirac Dr Tallahassee, FL, 32310, USA

Email: vanderlaan@magnet.fsu.edu

Abstract. The recent commissioning of the 36 T Series-Connected Hybrid Magnet at the National High Magnetic Field Laboratory has uncovered an undesirable consequence of using super critical helium for cooling of superconductors. This recent dry magnet cooling technology greatly reduces the LHe requirements of the magnet and may be utilized more frequently in the future. Because the supercritical helium does not complete a phase transition with the addition of heat, the fluid can quickly expand. The increased expansivity of supercritical helium over liquid helium for a given heat load is capable of creating larger pressure waves. The impact pressure for compressible helium gas flow is combined with the speed of sound for ideal gases to determine if a high-speed pressure wave is sufficient to explain the premature failure of the burst discs in the over-pressurization protection system. The addition of an impact pressure can explain, under the right conditions, a reduction of up to 40% in the burst disc pressure rating. The Grüneisen parameter is shown to relate to the expansivity and values for the parameter are given in the supercritical range. A proposal to reroute the pipe near the burst disc is made to mitigate the effects of the impact pressure.

1. Introduction

The Series Connected Hybrid (SCH) magnet at the National High Magnetic Field Laboratory consists of a Florida-Bitter resistive coil insert and a superconducting cable-in-conduit conductor (CICC) outsert. The insert and outsert are connected in series and with 20 kA are able to generate a magnetic field of 36 T with a homogeneity of 1 ppm in the sample volume [1, 2]. The SCH is cooled using a 17.3 g/s flow of 4 Bar supercritical helium at 4.8 K. Because the helium is supercritical instead of the standard liquid traditionally used for cooling magnets, the magnet is referred to as a dry magnet. Pressurized supercritical helium has been shown to have heat transfer rates of ~ 10 kW/m², which is comparable to pool boiling [3]. The use of dry magnet designs has increased because the helium usage can be decreased. For instance, the 45 T Hybrid magnet at the NHMFL uses ~ 280 W of cooling (via feeding a 1,750 L helium reservoir) for an 11 T outsert while the SCH uses ~ 120 W of cooling (via ~ 100 liquid liters of helium at super critical pressures) for a 13 T outsert. Due to an unstable helium market, increased helium prices are making dry magnets a more appealing option.

2. Premature failure

The disadvantages of dry magnet systems are still being discovered. Since late 2017 the SCH has operated as a user magnet. During this time several adjustments have been made to the cooling



parameters, quench detection limits, and quick-acting vent relief setpoints to help smooth operations. One of the largest operational hurdles involved the premature rupture of the burst discs.

Although it is safer for the discs to fail at a lower value than specifications, replacement after rupture was expensive, time consuming, and delayed magnet operations. The lock-out tag-out of all pressure and voltage sources into the SCH was used to safely access the burst disc, but it took a couple of hours to apply and remove. The costs of the lost helium and replacement rupture discs are substantial. Additionally, the magnet would be not run for the remainder of the day as the cooling system was recovered.

The SCH uses three protection devices in parallel: Quick-acting valves, resealing pressure relief valves, and burst discs [4]. Quick-acting valves connected to the magnet quench detection system were originally set at 6 Bar. The resealing pressure reliefs open at 12 Bar and the SCH burst discs are rated at 20 Bar. This arrangement provides pressure relief at various values and should reseal if the pressure is less than 20 Bar. However, a static pressure gauge tapped perpendicular to the flow indicated the burst discs were breaking at pressures as low as 12 Bar.

A design flaw in the burst disc causing the metal film to buckle at pressure below the set point was discovered following the premature failure. This observation significantly reduced confidence in future performance. Static pressure tests of the burst discs showed that the actual rupture pressure was more than 30% more than the set pressure. Downstream support rings were added, and the burst discs were retested. The modified burst discs correctly failed at 20 Bar. Even after this design issue was addressed the burst disc would continue to prematurely rupture at pressures of 10.7 Bar. A more in-depth examination was needed.

During a quench, the pressure generated inside the CICC can be enormous and hard to predict. At full field, the SCH can generate pressure waves with a static pressure of 10.7 Bar. Due to the perpendicular orientation, the pressure sensor only measures the static pressure. Measurement of additional dynamic pressure was not accounted for in the original design. However, the additional pressure it adds is responsible for the premature failure. Pressure sensors measure each of the three incoming lines (high-field, mid-field, and low-field) and the exit line. The pressure plot of a typical quench is shown in Figure 1.

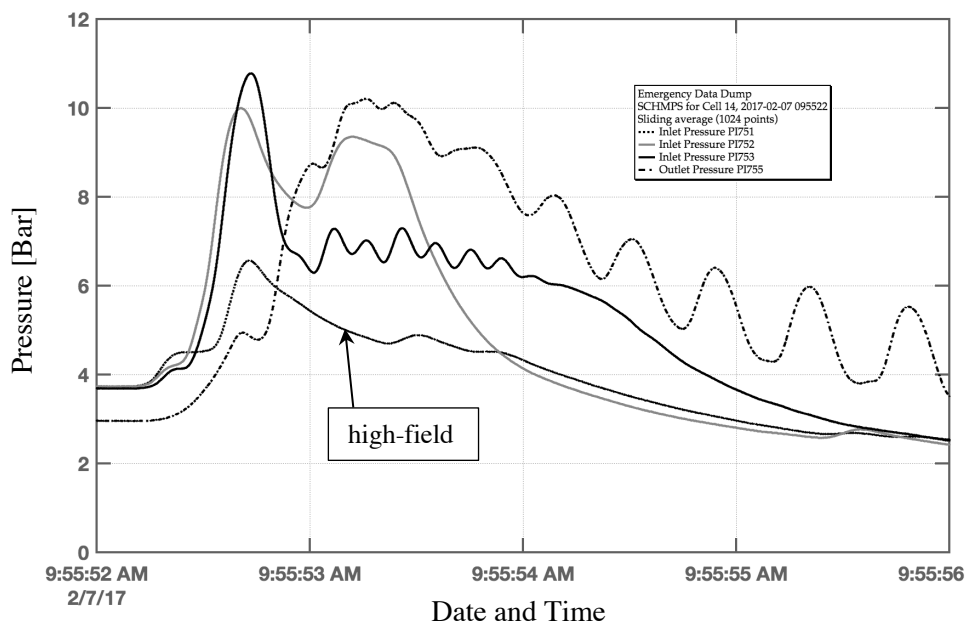


Figure 1. Pressure plots of SCH quenches

During this particular quench the burst disc in the high field cooling circuit broke. Although this circuit shows the lowest pressure, the actual pressure seen by the burst disc is believed to also be ~ 10.7 Bar. The pressure sensor does not record 10.7 Bar because it is downstream of the burst disc.

3. Theory

In order to explain the premature burst disc failure, the incompressible dynamic pressure in a one-dimensional isentropic flow is analysed for velocities less than 0.3 Mach.

$$P_d = \frac{1}{2} \rho v^2 \quad (1)$$

where ρ is the density and v is the velocity. At the conditions present in the SCH ($T = 4.8$ K, $P = 4.00$ BAR) the additional dynamic pressure of a Mach 0.3 pressure spike does not make a significant contribution to the static pressure. But helium quench speed inside CICC may exceed 0.3 M . In fact, the high speeds of a resulting pressure spike due to quench was proposed as a quench detection method in 1988 [5]. This method is currently being used on the SCH in parallel with the traditional voltage quench detection means [4] and also in use by others [6]. In the SCH, the pressure rise may happen as quickly as 0.1 second.

To examine velocities larger than 0.3 Mach, a compressible form of the impact pressure (also twice the dynamic pressure) must be considered. The stagnation pressure coefficient has previously been defined as

$$C_{po} = \frac{P_o - P}{\frac{1}{2} \rho v^2} \quad (2)$$

where P_o is the stagnation pressure and P is the static pressure. Equation 2 can be rewritten using the Newton-Laplace equation for the speed of sound in an ideal gas, using $\gamma = 5/3$ as the specific heat ratio for helium.

$$C_{po} = \frac{P_o - P}{\frac{1}{2} \gamma P M^2} = \frac{6}{5 M^2} \left(\frac{P_o}{P} - 1 \right) \quad (3)$$

The pressure ratio of the stagnation and static pressure ratios can be expressed in a one-dimensional isentropic flow along a streamline [7] as

$$\frac{P_o}{P} = \left[1 + \frac{\gamma - 1}{2} M^2 \right]^{\gamma / \gamma - 1} \quad (4)$$

When solved for helium the equation is reduced to

$$\frac{P_o}{P} = \left[1 + \frac{M^2}{3} \right]^{5/2} \quad (5)$$

Using the Binominal Theorem the previous Equation 5 can be expanded to

$$\frac{P_o}{P} = 1 + \frac{5M^2}{6} + \frac{5M^4}{24} + \frac{5M^6}{432} \dots \quad (6)$$

The stagnation pressure coefficient can then be added to the expanded stagnation and static pressure ratio

$$C_{po} = 1 + \frac{M^2}{4} + \frac{M^4}{72} + \dots \quad (7)$$

Plugging this back into the stagnation pressure coefficient definition gives the impact pressure for compressible helium flows

$$P_o - P = \frac{1}{2} \rho v^2 \left[1 + \frac{M^2}{4} + \frac{M^4}{72} + \dots \right] \quad (8)$$

$$P_o - P = \frac{1}{2} \gamma P M^2 \left[1 + \frac{M^2}{4} + \frac{M^4}{72} + \dots \right] \quad (9)$$

which is valid for $M < 1$. The presence of shock waves would disrupt the streamline assumption made on Equation 4.

At the extreme limit of these equations, consider a velocity of $M = 1$. Equation 6 then reduces the impact pressure to a temperature-independent relationship as the density component cancels out. With some algebra it can be rewritten as

$$P = \frac{P_o}{\frac{5}{6} \left[1 + \frac{1}{4} + \frac{1}{72} + \dots \right] + 1} = \frac{P_o}{2.053} \quad (10)$$

This means that for flows of $M = 1$ the stagnation pressure can be more than twice the amount of the static pressure. Under these conditions a rupture disc rated for 20 Bar can break while measuring approximately 9.74 Bar on the static pressure gauge.

The quench on the SCH created conditions of a 10.8 Bar static pressure and at least a 20 Bar stagnation pressure to rupture the disc. Solving Equation 6 in combination with the Laplace-Newton equation under these conditions leads to a pressure wave speed of $M = 0.74$. A theoretical prediction of pressure wave velocities is complex and would involve several assumptions [8]. The experimentally calculated velocity seems reasonable and achievable.

4. Grüneisen parameter for supercritical helium

The above equations show that it is possible to produce impact shocks with velocities lower than Mach 1. The question then becomes how to avoid the unwanted pressure impact. Magnets utilizing pool boiling have not produced such large impact pressures because the heat from the quench is largely absorbed by the latent heat of helium ($H_L = 21$ kJ/kg) during the phase transition. Per mass this has the same heat absorbance as approximately a 4 K temperature rise [9]. When forced flow supercritical helium is used instead, the operating point is above the phase transition and therefore all heat deposited will result in a rise in temperature and fluid expansion [10].

To examine the change in specific volume and the heat deposited to the fluid via enthalpy change, the Grüneisen parameter for supercritical helium is determined. The Grüneisen parameter has been defined in several ways. The simplest definition is the ratio between the volumetric thermal expansivity β and the specific heat C_p [11].

$$\Gamma = \beta / C_p \quad (11)$$

By substituting known relations for both volumetric thermal expansivity β and the specific heat C_p under constant pressure [12, 13], Equation 11 can be rewritten as

$$\Gamma = \beta / C_p = \rho \left(\frac{\delta v}{\delta T} \right)_P / \left(\frac{\delta h}{\delta T} \right)_P = \rho \left(\frac{\delta v}{\delta h} \right)_P \quad (12)$$

where v is the specific volume and h is the enthalpy. Under this rearrangement, the Grüneisen parameter can be used to compare the change in specific volume compared to the enthalpy added to the fluid.

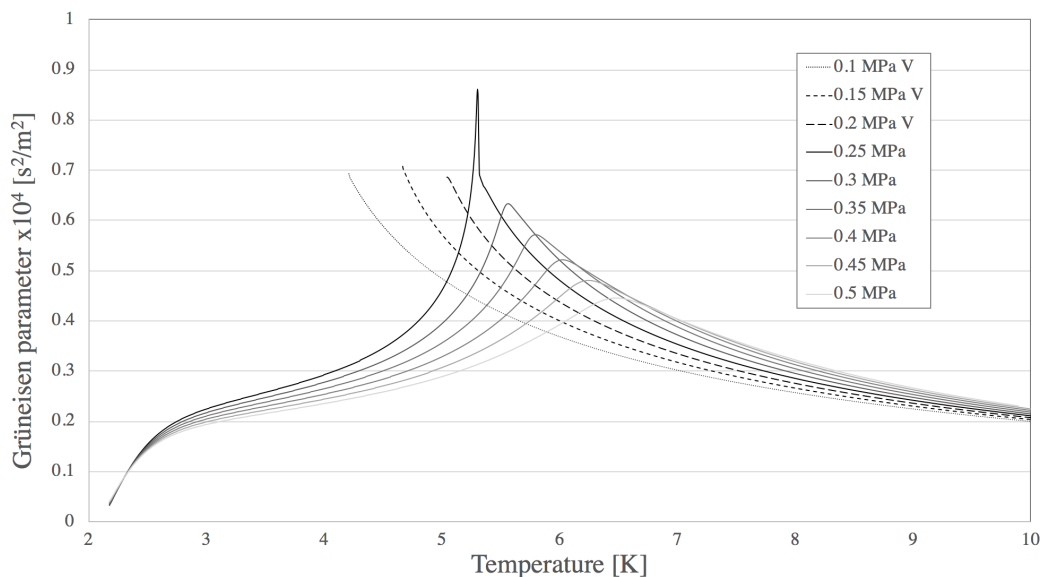


Figure 2. Grüneisen parameter for helium near critical point

To reduce the pressure wave propagation speed, high Grüneisen numbers should be avoided. Using NIST REFProp version 10 [14], the Grüneisen parameter for supercritical helium and gas helium for pressures ranging from 0.1 – 0.5 MPa and temperatures from 3 – 10 K are shown in Figure 2.

Only supercritical and gas state helium are included. The Grüneisen parameter appears to diverge near the critical temperature and spikes near the critical pressure. This is to be expected as supercritical helium is known to be volatile and unstable. Therefore, the Grüneisen parameter should be the largest near the critical point ($T_c = 5.19$ K, $P_c = 2.24$ Bar). The kink in this data may be due to larger errors in the NIST data near the critical point.

5. Future work

Currently, the burst discs are connected to the helium space via a 30-inch long straight pipe with diameters varying from 0.92 – 1.37 inch. This straight pipe arrangement was chosen to reduce the pressure drop between the pressurized gas and the vent, which is good practice. For dry magnet purposes a new configuration (Figure 3) is proposed to reduce the impact pressure effects on burst discs.

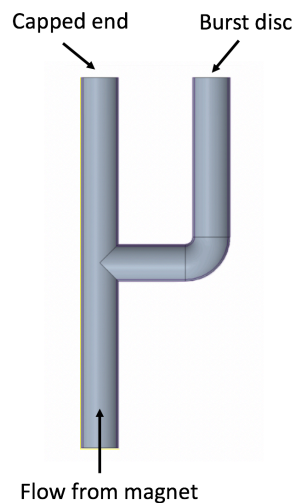


Figure 3. Impact pressure diffuser

This new burst disc configuration should reduce the impact pressure on the burst disc as the pressure wave no longer has a straight and direct path to the burst disc. This configuration should result in the burst disc experiencing a pressure closer to that of the static pressure. This configuration should also maintain the flow capacity of the burst disc as the outlet vent area is unchanged and the slightly larger pressure drop due to minor losses in the bend will not reduce the already choked flow of the venting helium.

The pressure drop of the proposed inlet line produces approximately 0.8 psi pressure drop which is less than 3% of the burst disc rating. This impact-resistant burst disc setup is still in agreement with both ASME Section VIII Pressure Vessel Code [15] and the Compressed Gas Association S-1.3 Pressure Relief Device Standards [16].

6. References

- [1] Chen J, Cantrell K, Bai H, Bird M, and Bole S 2011 *IEEE Trans. Appl. Supercond.* **21**, 2118.
- [2] Bird M, Brey W, Cross T, Dixon I, Griffin A, Hannahs S, Kynoch J, Litvak I, Schiano J, and Toth J 2018 *IEEE Trans. Appl. Supercond.* **28**, 4300706.
- [3] Giarratano P, Arp V, Smith R 1971 *Cryogenics* **11**, 385.
- [4] Bai H, Bird M, Bole S, Cantrell K, Dixon I, Gavrilin A, Painter T, Xu Ting 2010 *AIP Conf.*

- Proc.* **1218**, 1231.
- [5] Desner L 1988 *Adv. Cryog. Eng.* **33**, 167.
 - [6] Sharma A, Pradhan S, Prasad U, Varmora P, Khristi Y, Doshi K, and Patel D 2015 *J. Fusion Energ.* **34**, 331.
 - [7] Houghton E, Carpenter P 2003 *Aerodynamics for Engineering Students 5th Edition* (Burlington: Butterworth-Heinemann) p 278.
 - [8] Babitch V, Churbanov V, Schmidt C, Tateishi H 1991 *Cryogenics* **31**, 645.
 - [9] Van Sciver S 2012 *Helium Cryogenics* (New York: Plenum Press)
 - [10] Schmidt C 1988 *Cryogenics* **28**, 585.
 - [11] Souza M, Menegasso P, Paupitz R, Seridonio A, Lagos R 2016 *Eur. J. Phys.* **37**, 055105.
 - [12] Schroeder D 1999 *An Introduction to Thermal Physics* (San Francisco: Addison Wesley Longman) p 34.
 - [13] Arp V 1975 *Cryogenics* **15**, 285.
 - [14] Lemmon E, Bell I, Huber M, and McLinden M. NIST Standard Reference Database 23: Reference Fluid Thermodynamic and Transport Properties- REFPROP, Version 10.
 - [15] ASME Boiler and Pressure Vessel Code, VIII Rules for Construction of Pressure Vessels, 2013.
 - [16] Compressed Gas Association, CGA S-1.3, Pressure Relief Device Standards Part 3, 2008.

Acknowledgments

Thank you to Edwin Diaz for help with the Binominal Theorem. This work was performed at the National High Magnetic Field Laboratory, which is supported by NSF DMR-1644779 and the State of Florida.